JOURNAL OF APPLIED ELECTROCHEMISTRY **28** (1998) 1021–1033

REVIEWS IN APPLIED ELECTROCHEMISTRY, NUMBER 50

# Electrodes based on Magnéli phase titanium oxides: the properties and applications of Ebonex® materials

J. R. SMITH*, F. C. WALSH

*Applied Electrochemistry Group, University of Portsmouth, St. Michael's Building, White Swan Road, Portsmouth PO1 2DT, Great Britain*

R. L. CLARKE

*EDA Technology, 829 Heinz Street, Berkeley, CA 94710, USA*

Received 21 October 1997; accepted in revised form 23 February 1998

Magnéli phases are a range of substoichiometric oxides of titanium of the general formula $Ti_nO_{2n-1}$, (where $n$ is between 4 and 10) produced from high temperature reduction of titania in a hydrogen atmosphere. These blue/black ceramic materials exhibit a conductivity comparable to that of graphite and can be produced in a number of forms, such as tiles, rods, fibres, foams and powders. While these materials have been studied for many years, they have only recently received interest for use as ceramic electrode materials, commercially termed 'Ebonex®', and are beginning to challenge precious metal coated anodes for some applications in aggressive electrolytes. Other uses for these materials include electrowinning, electroplating, battery materials, impressed current cathodic protection anodes, electrochemical soil remediation, oxidation of organic wastes, flexible cable materials and electrophoresis. The scope of this review considers the structure and properties of Magnéli phase titanium oxide materials, together with their electrochemical behaviour and applications.

Keywords: *Magnéli phases*, *substoichiometric*, *conductive*, *titanium oxides*

## Nomenclature

*Symbols*

| | |
|---|---|
| $dE/dT$ | potential scan rate (mVs$^{-1}$) |
| $j$ | current density (mA cm$^{-2}$) |
| $E_e^\circ$ | Standard redox potential (mV) |
| $E_p^c$ | cathodic peak potential (mV) |
| $E_p^a$ | anodic peak potential (mV) |
| $\Delta E_p$ | peak separation potential difference (mV) |
| $T$ | temperature (K) |
| $\alpha, \beta, \gamma$ | angles between cell parameters (deg) |
| $\sigma$ | conductivity (S cm$^{-1}$) |

*Abbreviations*

| | |
|---|---|
| a, b, c | cell parameters |
| AFM | atomic force microscopy |
| CV | cyclic voltammogram |
| SCE | saturated calomel electrode |
| SEM | scanning electron microscopy |
| STM | scanning tunnelling microscopy |

*Compounds*

| | |
|---|---|
| $IrO_2$ | iridium dioxide |
| $PbO_2$ | lead (IV) oxide |
| $RuCl_3$ | ruthenium (III) chloride |
| $RuO_2$ | ruthenium (IV) oxide |
| $Sb_2O_3$ | antimony (III) oxide |
| $SnO_2$ | tin (IV) oxide |
| $TiO_2$ | titanium (IV) oxide |
| $Ti_nO_{2n-1}$ | nonstoichiometric, Magnéli phase titanium oxides |
| $TiO_x$ | nonstoichiometric titanium oxides (not necessarily Magnéli phases) |

## 1. Introduction

Magnéli phases are a substoichiometric composition of titanium oxides of the general formula $Ti_nO_{2n-1}$, where $n$ is a number between 4 and 10 (Fig. 1) [1]. They are identifiable compounds and not simply doped titania or casual mixtures of $TiO_x$, where $x$ is less than 2 [2]. The magnetic and electrical properties of these phases have been widely investigated [3–7], although their use as electrode materials is more recent [8–12]. Here, the structure, physical properties and electrochemical behaviour of Magnéli phases, commercially known as 'Ebonex® materials', are reviewed and their uses in electrochemical processing and device manufacture are discussed. The development of modified mate-

---

* Address for correspondence: Scanning Probe Microscopy Laboratory, University of Portsmouth, Portsmouth, PO1 2DT, UK.

0021-891X

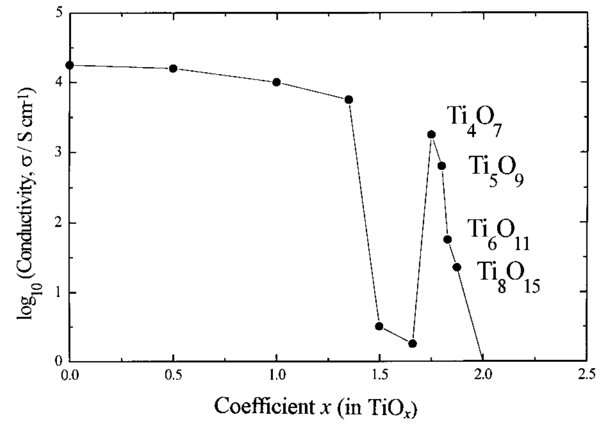

Fig. 1. Phase diagram of the titanium–oxygen system, showing stoichiometry of the titanium oxides against the log of conductivity of oxide phases [2].

rials (e.g., coated and flexible, Ebonex®) is also considered.

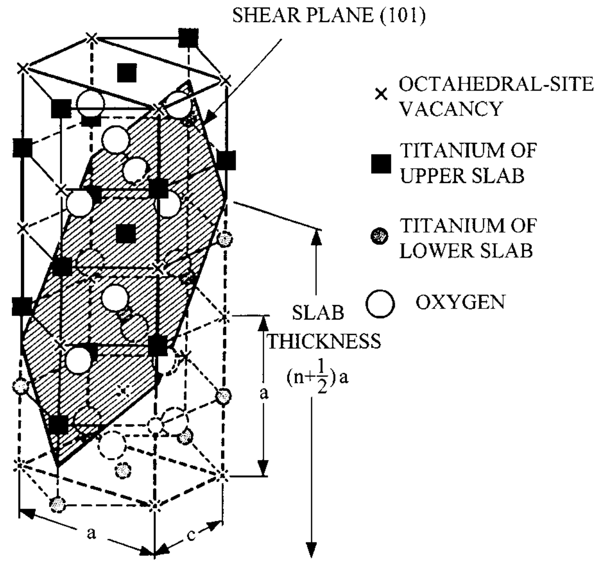

Fig. 2. Unit cell projection of the shear plane in the Magnéli phase $Ti_4O_7$. c, a and (1 0 1) refer to axes of rutile slabs [6].

## 2. Structure and physical properties

Until the 1959s, titanium oxide was thought to exit in a wide-range of nonstoichiometric forms. However, such structures were considered energetically unfavourable due to the congregation of lattice defects into planes that would collapse and alter their structure, resulting in the formation of distinct phases. The X-ray crystallographer, Magnéli, was first to study these materials based on rutile, $TiO_2$, which are now called Magnéli phases [1].

Each of the Magnéli phases has a distinct and recognisable XRD pattern. Table 1 shows the unit cell parameters for each of the main phases. Discontinuities in some of the data arise due to different choices of space groups selected by different authors for calculation of the XRD patterns. In general, the calculated results are in very good agreement with those obtained experimentally [13–16].

The phases are made up of two dimensional chains of titania octahedra, with every *n*th layer having oxygen atoms missing to accommodate the loss in stoichiometry. Thus, $Ti_4O_7$ can be considered as being made up of three $TiO_2$ octahedra and one TiO octahedra; in the TiO layer, titanium atoms are closer together than in other parts of the lattice due to oxygen vacancies creating an edge, rather than a corner joining and a shear plane along the TiO chains (Fig. 2) [6, 17]. The geometrical basis for the sequence $Ti_{10}O_{19}$–$Ti_4O_7$ is the increased face sharing of oxygen atoms between $TiO_6$ octahedra rather than edge and corner sharing as the number of octahedra across a block diminishes. Figure 3 shows the location of crystal shear planes in Magnéli phases in the (1 0 1), (1 1 0), (1 2 1) and (1 3 2) planes [18].

*Table 1. Unit cell parameters for some of the Magnéli phase titanium oxides $TiO_{(2-x)}$*

| *Phase* | *a* | *b* | *c* | *α* | *β* | *γ* | *Ref.* |
|---|---|---|---|---|---|---|---|
| $Ti_4O_7$ | 5.600 | 7.133 | 12.466 | 95.05 | 95.17 | 108.71 | [13] |
| $Ti_5O_9$ | 5.569 | 7.126 | 8.865 | 93.17 | 112.34 | 108.50 | [14] |
| $Ti_6O_{11}$ | 5.552 | 7.126 | 32.233 | 66.94 | 57.08 | 108.51 | [15] |
| $Ti_7O_{13}$ | 5.537 | 7.132 | 38.151 | 66.70 | 57.12 | 108.50 | [15] |
| $Ti_8O_{15}$ | 5.526 | 7.133 | 44.057 | 66.54 | 57.18 | 108.51 | [15] |
| $Ti_9O_{17}$ | 5.524 | 7.142 | 50.03 | 66.41 | 57.20 | 108.53 | [15] |

Several oxides from the homologous series, principally $Ti_4O_7$ and $Ti_5O_9$, exhibit high electrical conductivity at room temperature [4, 19] (Fig. 1). For example, $Ti_4O_7$, the most highly conductive phase [4], exhibits a single crystal conductivity of 1500 S cm$^{-1}$ [5, 8], comparable to that of graphite (Table 2) [20]. Magnetic susceptibility studies [7, 21–23], differential thermal analysis and conductivity measurements [4] have revealed semiconductor-to-mental transitions in several of the phases. The electrical conductivity of $Ti_4O_7$ can be explained in terms of a hopping mechanism for temperatures below the transition, with

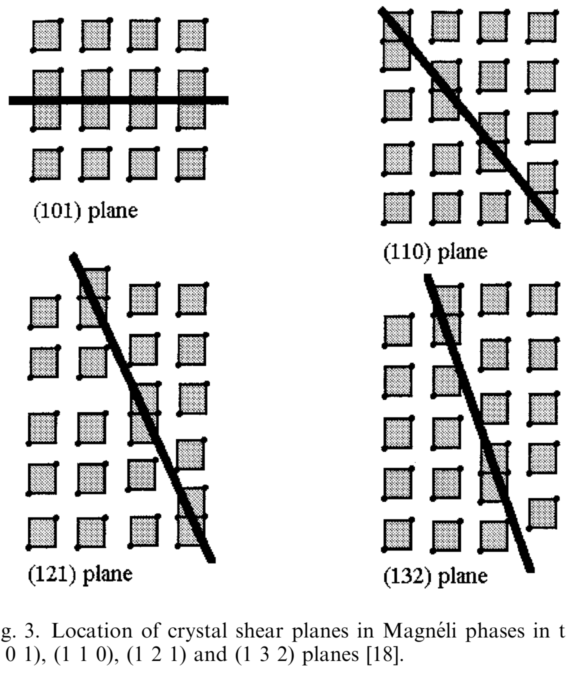

Fig. 3. Location of crystal shear planes in Magnéli phases in the (1 0 1), (1 1 0), (1 2 1) and (1 3 2) planes [18].

*Table 2. Comparative resistivities of some electrode materials* [2]

| *Material* | *Resistivity* /$\mu\Omega$ cm |
|---|---|
| Copper | 1.7 |
| Aluminium | 2.7 |
| Lead | 20.6 |
| Tianium | 45 |
| $Ti_4O_7$ | 630 |
| Carbon (graphite) | 1375 |

optical mode phonon scattering and ionised defect scattering dominating above the transition [3]. In low temperature phases, pairs of $Ti^{3+}$ ions are separated by short covalent metal–metal bonds arising from the overlap of the 3d electrons. Above the transition temperature (149 ± 2 K in the case of $Ti_4O_7$ [4]), these bonds break as the Ti–Ti distances suddenly increase and the 3d electrons then participate in metallic conduction [24]. This is evidenced by a concomitant increase in magnetic susceptibility [22, 25] and an increase conductivity by three orders of magnitude [4]. The actual value of the conductivity of a given sample is a function of the particular Magnéli phase present and the method by which it is made [26]. The density of the material and the presence of pores and microcracks can significantly effect conductivity as well as the corrosion resistance and strength of the ceramic. The presence of impurities, such as aluminum oxide, reduces the corrosion resistance of the material, especially in alkaline media [26].

## 3. Manufacture

Magnéli phases are produced from titanium dioxide ($TiO_2$), one of the most abundant, pure materials available, which is widely used in ceramics manufacture and as a white pigment in paints, paper and foodstuffs. Typically, the material is heated to temperatures exceeding 1273 K and allowed to cool to ambient temperature under a controlled atmosphere of hydrogen. These high temperature are necessary ensure that Brookite and Anatase forms of titania are not formed, as the are relatively noninert, being digested in mineral acids. In a typical production method, a mixture of water and isopropanol (1:1) is added to titania to minimise capillary forces in the powder and, after drying, a 5% by weight polyethylene oxide solution is added as a binder [27]. The powders are compressed in a uniaxial press under a pressure of 200 kg $cm^{-2}$ to the desired shape and the resultant blocks sintered in air at 1323 K for one day. After removal of oxygen from the furnace, reduction is carried out using hydrogen gas to obtain monophasic $Ti_4O_7$ after 4 h at 1323 K. Higher oxides can also be produced by shortening reduction times. Materials with variations in pore size distribution can be made through the use of porosity agents, such as carbon, and different grain sizes of $TiO_2$ powders and changing the sintering and reducing conditions. Table 3 shows some typical properties of porous and non-permeable grades of commercially available Magnéli phase materials.

## 4. Magnéli phases as ceramic electrodes

The high conductivity and chemical stability of Magnéli phases has attracted interest from electrochemists and electrochemical engineers, such that Ebonex® materials have been used both as an electrode material in their own right and as a support for various electrocatalysts [28, 29]. The development of electrochemical applications of such materials can be traced to early work by Hayfield and Clarke [30].

Before the use of Magnéli phases as electrode materials, a number of bulk ceramic materials, such as the spinels and perovskites, were studied for use as corrosion resistant electrodes in electrochemical applications [31–33]. However, these were only successful in limited circumstances. Ferrites were commercially used as cathodic protection anodes and electrodes for some effluent treatment and water sterilisation processes but they have low conductivity and stability. Sodium tungsten bronzes [13, 14] were proposed as alternatives to platinum catalysts in fuel cells and some success was achieved using precious metal oxide coated titanium.

Magnéli phases are usually more corrosion resistant in very aggressive conditions than conventional

*Table 3. Physical properties of two grades of commercially available Magnéli phase ceramic materials* [26]

| *Physical property* | *Porous grade* | *Nonpermeable grade* |
|---|---|---|
| Chemical formula | $Ti_4O_7/Ti_5O_9$ | $Ti_4O_7/Ti_5O_9$ |
| Appearance | Blue–black, odourless solid | Blue–black, odourless solid |
| Boiling point/°C | > 3000 | > 3000 |
| Melting point/°C | 1850 | 1850 |
| Bulk resistivity/$\Omega$ $cm^{-1}$ * | (20–40) × $10^{-3}$ | (1–10) × $10^{-3}$ |
| Bulk density/g $cm^{-3}$ | 3.6–3.8 | 3.9–4.2 |
| Porosity/% | 20 | 0.1–4.0 |
| Flexural strength/MPa | 60–180 | 160–300 |
| Hardness/(Vickers) | 230 | Not applicable |
| Specific heat capacity/J $kg^{-1}$ | 0.75 | – |
| Thermal conductivity/W $m^{-1}$ $K^{-1}$ | 10–20 | – |
| CAS numbers | 12 143–55–4, 12 065–98–4, 12 143–56–5, 12 143–58–7 | |

* Measured using a four-point conductivity probe [26].

electrode materials used in large electrochemical processing industries; the ceramic is more chemically stable than the parent metal, titanium and even titania. The ceramic is particularly stable in etchants containing fluoride, hydrochloric acid and aqua regia. Titanium is conventionally etched using concentrated hydrochloric acid at ambient temperature, typically using 40% sulphuric acid at 333 K or oxalic acid at 353 K. However, Magnéli phase are inert to these aggressive etchants, although some materials are slowly corroded in boiling phosphoric acid, concentrated hydrofluoric acid at elevated temperature and sodium hydroxide solutions in excess of 12 mol dm$^{-3}$.

Ceramic materials, made in high temperature furnaces are likely to be in their most stable, fully oxidized form and therefore unlikely to undergo further oxidation. Metals and carbon do not possess this stability to oxidation but are electrically conductive. Magnéli phases combine the high conductivity of metals with the desirable corrosion resistant properties of ceramic materials.

Hayfield first discussed the unusual electrochemical properties of the Magnéli phases and subsequently patented the manufacture and uses of these oxides in electrochemistry [30]. He named the products made from the ceramic 'Ebonex®' materials. The name is now a registered trade mark of Atraverda Ltd (Sheffield, UK). Electrodes are usually constructed from commercially available sheets which are cut into discs using a diamond tool [34]. Silver-loaded epoxy can be used to make an electrical contact to a copper wire and the electrodes encapsulated in glass tubes using epoxy resin. For rotating disc electrodes, ceramic discs can be directly mounted on the stainless steel unit to be connected to the rotating motor and sealed within a Teflon® sheath; the electrode can then be ground on silicon carbide paper to expose the ceramic surface.

Advanced ceramic processes are able to produce Ebonex® materials in a variety of three-dimensional forms, such as rods, tubes, complex extruded shapes, fibres, pellets and powders, in addition to the more usual tile and sheet forms. Powders are particularly useful, since variations in particle diameter affect surface area, a useful parameter in the optimal control of electrochemical flow-cells and reactors. FM01-LC electrodes (nominal area 16 cm × 4 cm) [35, 36] have been fabricated by a proprietary process which places an Ebonex® coating on metallic substrates and on plate and reticulated Ebonex® materials [37, 38].

Preliminary microscopic characterization of porous Ebonex® materials has been carried out using scanning electron microscopy (SEM) [34]. Surfaces appeared microrough, and despite the sample being termed 'nonporous', there are many small pores present. Figure 4 shows typical SEM micrographs of some three-dimensional forms of Ebonex® electrodes. Fibres are of uniform diameter and possess a homogeneous structure (Fig. 4(a)), of similar appearance to the porous tile material (not shown). The powdered form has a very jagged morphology (Fig. 4(b)) and can be manufactured to various average particle sizes (approximately 5 $\mu$m shown here). Figure 4(c) shows the characteristic 'Y'-shaped junction between three aveoli in a reticulated Ebonex® material. The diameter of each aveolus in this sample is approximately 700 $\mu$m.

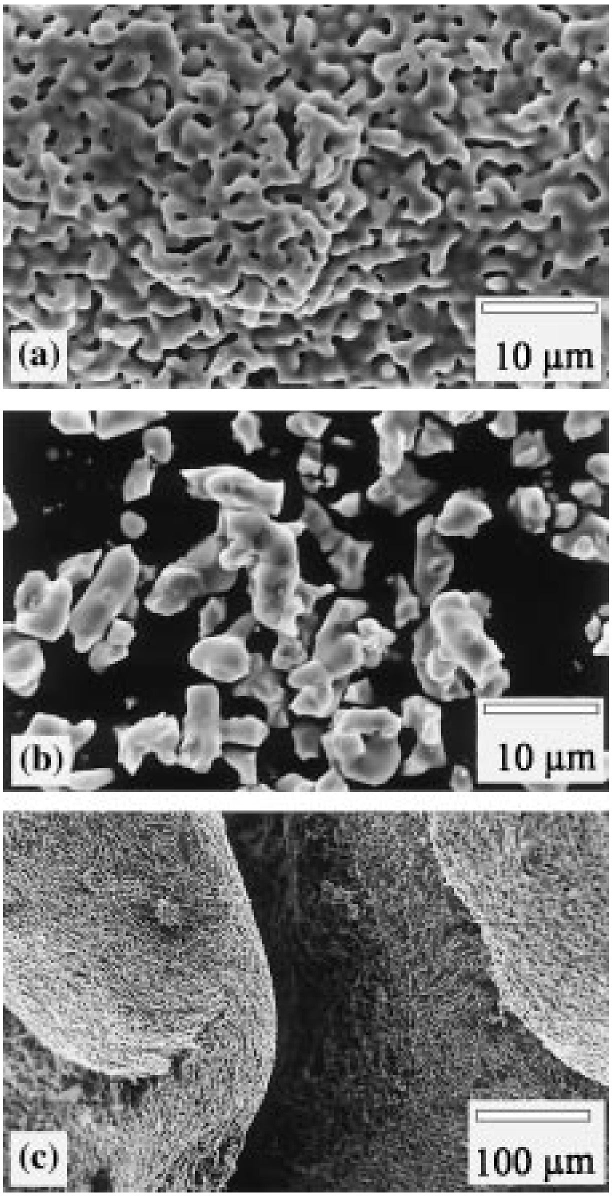

Fig. 4. Scanning electron micrographs of various three dimensional forms of Ebonex® materials: (a) fibre, (b) powder, and (c) reticulate.

Scanning probe microscopy (SPM) techniques, such as atomic force microscopy (AFM) and scanning tunnelling microscopy (STM), have also recently been used to investigate the topography of porous and fully-hardened (nonporous) Ebonex® materials at high resolution (Fig. 5) [39]. The porosity of the former was found to range from 12 to 15% by volume in agreement with water immersion measurements [40], as quoted by manufacturers [41].

A recent development has been the manufacture of conductive plastics in which various polymers have been impregnated with Ebonex® ceramic powders

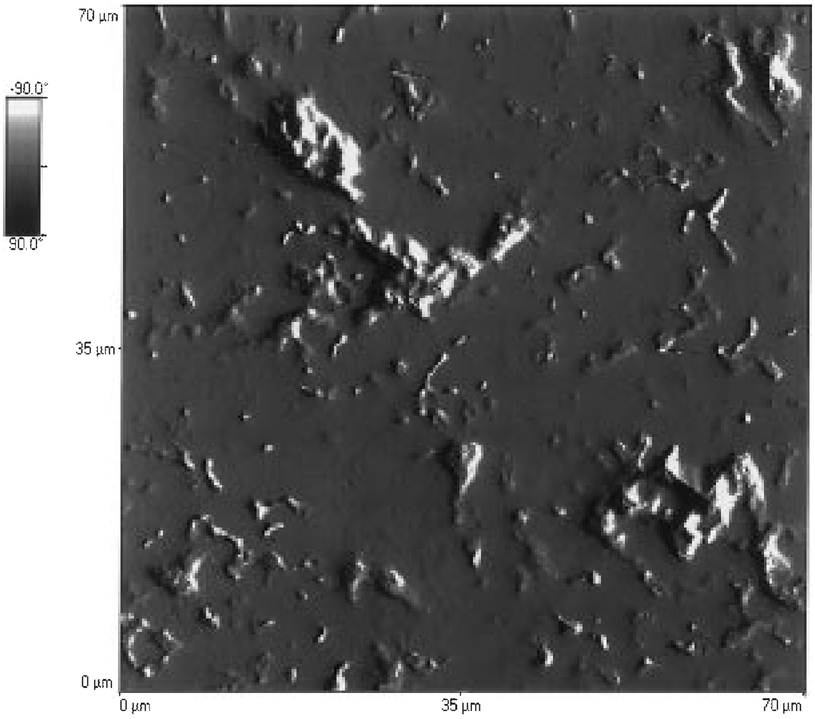

Fig. 5. An atomic force micrograph of a typical porous Ebonex® electrode. Image obtained in contact mode in air using a standard profile silicon nitride tip, 200 $\mu$m length 'V-shaped' cantilever of spring constant 0.038 $\mathrm{N\,m^{-1}}$ and a force of 5 nN [39].

[42]. It is possible to fill polyethylene and other polymers to a point where the material is a polymer bound particulate matrix rather than a randomly filled plastic. At a filling level of 85% by weight, the conductive material behaves like the ceramic with respect to its electrochemical properties, although it retains the toughness and desirable properties of the polymer. Figure 6 shows an AFM micrograph of a 'flexible' Ebonex® electrode development, a composite material containing 85% by weight Ebonex® powder in a polyethylene matrix. The powder can be seen as the dispersed phase, although in this material, the ohmic contact of particulates is insufficient to provide high conductivity. Flexible Ebonex® materials are not as conductive as the bulk ceramic, but this can be improved with metal inserts which can be used to provide high current carrying capabilities down the length of the plastic.

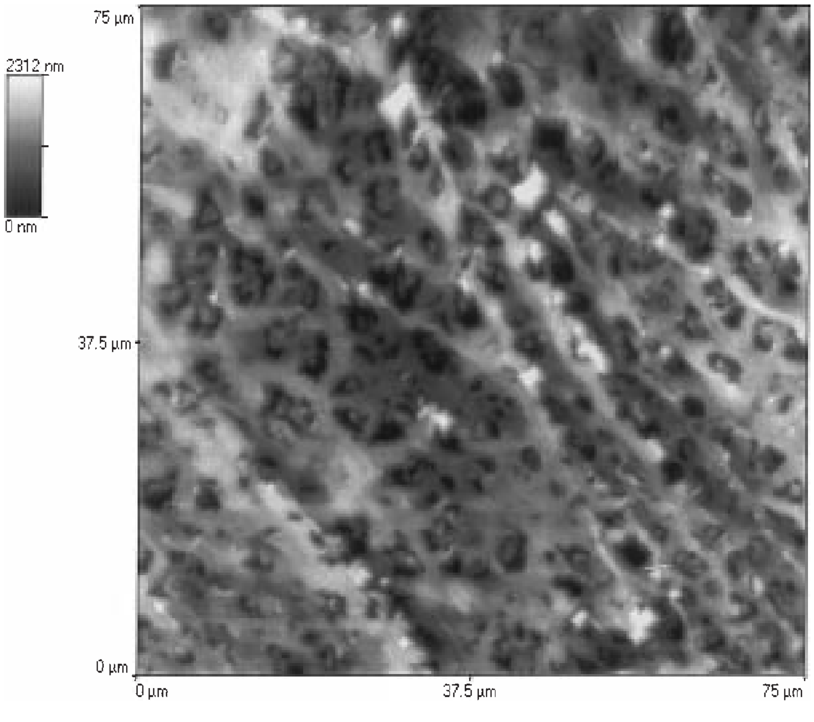

Fig. 6. Atomic force micrograph of a 'Flexible' Ebonex® electrode development, a composite material containing 85% by weight Ebonex® powder in a polyethylene matrix. Imaging parameters same as those stated for Fig. 5.

## 5. Electrochemistry of Ebonex® materials

The cyclic voltammogram of an Ebonex® plate electrode in 1 mol dm$^{-3}$ sulphuric acid at 298 K (Fig. 7) shows broad, poorly defined oxidation and reduction peaks, which have been attributed to changes in the oxidation state of titanium at the surface [11]. Background currents are sometimes observed, particularly on the first cycle. These may be attributed to a combination of high charging currents, resulting from the high porosity of the material, and some redox processes at the surface. X-ray diffraction studies show that $TiO_2$ is formed at Ebonex® electrode surfaces which have been subjected to very highly anodic potentials [11]. Results from polarization experiments in 1 mol dm$^{-3}$ sulphuric acid at 298 K show practical working current densities can be achieved in the range of 5 to 20 mA cm$^{-2}$ and that Ebonex® electrodes can operate as either anodes or cathodes, resulting in oxygen or hydrogen evolution reactions, respectively [26].

Uncoated Ebonex® anodes have a very high oxygen evolution overpotential and will passivate if the current exceeds 100 A m$^{-2}$ in a 1 mol dm$^{-3}$ sulphuric acid electrolyte. The ceramic electrode is a very poor catalyst for the promotion of oxygen evolution; the electrode potential increases above 5 V in many electrolytes at modest current densities at room temperature [26]. Some passivation of the surface occurs, usually in the form of lesser conductive Magnéli phases which show up in XRD studies. The presence of a small amount of electrocatalyst radically alters this behaviour and the ceramic can support current densities as high as 400 A m$^{-2}$ with very modest amounts of electrocatalyst, for example, 15 g m$^{-2}$ of iridium oxide (Fig. 8) [9, 11]. Much of the electrocatalyst penetrates the ceramic surface easily. Ebonex® materials have been coated with $PbO_2$ for ozone generation [34] and $RuO_2$ for oxygen evolution [43]. Ru–$Ti_4O_7$ has also been used as a microelectrode for the oxidation of $I^-$ to $I_2$ and $IO_3^-$ in 0.1 mol dm$^{-3}$ sulphuric acid at 298 K [44].

Ebonex® electrodes are sufficiently stable to be used as anodes or cathodes for water hydrolysis [9]. It is a more suitable material than carbon and vitreous carbon electrodes in that it does not decompose at high pH. However, between 50 and 100% greater overpotentials are necessary for hydrogen evolution (the actual value being dependent on pH) relative to Pt-black electrodes. It has been reported that soaking Ebonex® electrodes in a neutral solution of $RuCl_3$ significantly reduces the overpotential required for hydrogen evolution in acid electrolytes [9].

The electrochemical behaviour of simple redox species, such as ferro-/ferricyanide ion, hydroquinone, catechol, phenol and iodide, on Ebonex® materials show very slow kinetics and substantial overpotentials are necessary to drive oxidation and reduction reactions (Table 4) [11, 34, 45]. Only the ferro-/ferricyanide ion couple is active, but with a low current density of less than 0.8 mA cm$^{-2}$ (Fig. 9(b)) [9, 10, 45]. However, the kinetics of the redox couple are rapid when Ebonex® materials are electroplated with a suitable metal, such as platinum (Fig. 9(c)).

The porosity of Ebonex® electrodes has been shown to have a marked affect on their electrochemical behaviour [27], with the shape of the cyclic voltammogram (CV) and potentials of the oxygen

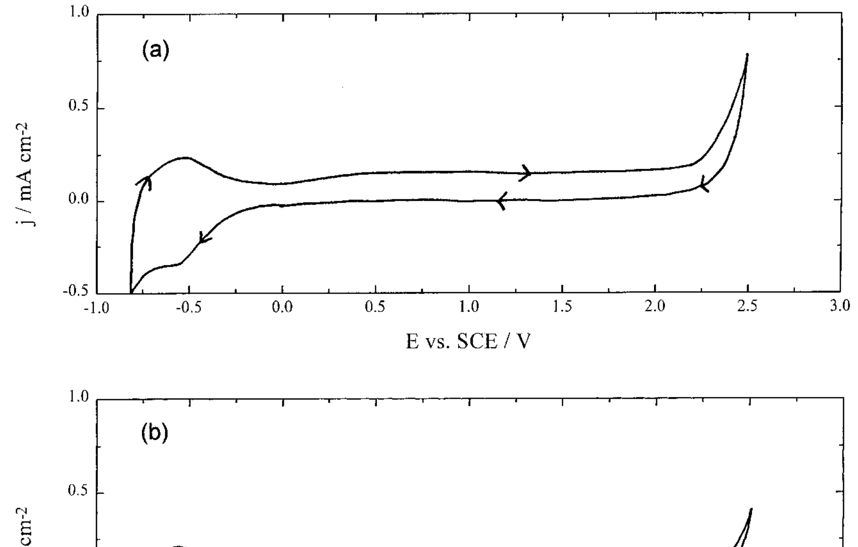

Fig. 7. Electrochemical behaviour of an Ebonex® material in 1 mol dm$^{-3}$ sulphuric acid: (a) 1st scan commencing at 0 V and scanning to negative potentials, and (b) 2nd scan, 0 V to positive potentials. $dE/dT = 50\,mV\,s^{-1}$; $T = 298\,K$ [11].

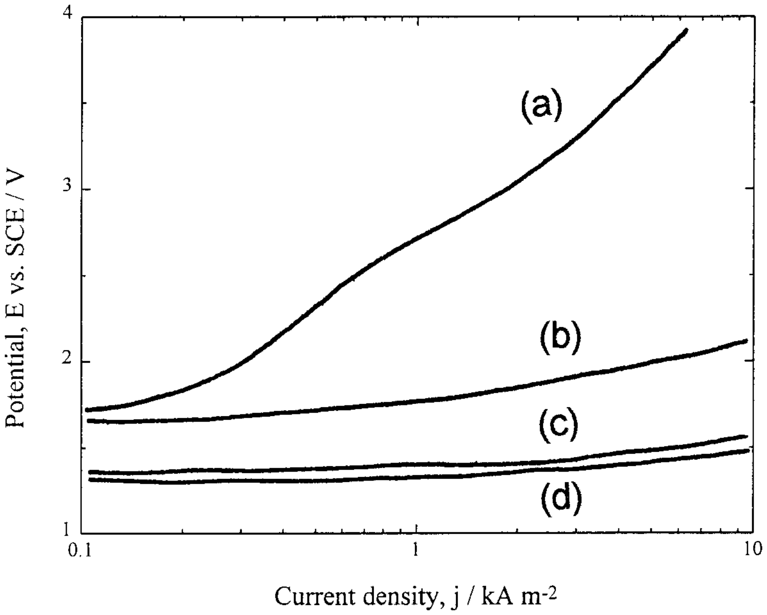

Fig. 8. Typical polarization curves for catalysed and uncatalysed Ebonex® electrodes in 1 mol dm$^{-3}$ sulphuric acid: (a) uncoated Ebonex®, (b) Pt/Nb substrate, (c) $IrO_2$/Ebonex® and (d) $IrO_2$/Ti [26].

and hydrogen evolution reactions being strongly dependent on pore size distribution of the ceramic electrodes. For example, the onset of the oxygen evolution reaction has been shown to increase from +2.5 to +2.8 V *vs*. SCE on going from a material containing many large pores to one containing a small number of small pores [27]. In addition, the most reproducible CVs and largest current densities are displayed by electrodes containing many large pores.

The high overpotential required for hydrogen and oxygen evolution [9] makes the material suitable for the cathodic deposition of metals, such as copper, gold, nickel, palladium and platinum, which adhere very strongly to Ebonex® surfaces [11]. Table 5 shows some typical electroplating bath conditions for the deposition of these metals on Ebonex® materials. Electrodeposition of a 1 $\mu$m thick layer of copper has been shown to produce crystallites of copper within the pores. Thicker deposits, of about 50 $\mu$m, involved crystallites which had completely overlapped to form a continuous film. Energy dispersive X-ray analysis of a cross section showed that copper deposition occurred deep inside the pores of the material. AFM has also used to study the early stages of copper electrodeposition on porous Ebonex® electrodes. Initial copper nucleation and growth were found to occur preferentially at surface pores of the material [39].

## 6. Applications

The introduction of Ebonex® ceramics into commercial applications has been slow, despite its outstanding electrochemical performance. This is most likely due to cost, resulting from a combination of factors: energy costs inherent in a batch process; capital barriers in scale-up to semicontinuous solid ceramic manufacture and costs associated with manufacturing durable connections in high anodic current density applications. However, Ebonex® materials are currently being explored for a diverse range of technological applications, such as chlorine generation, sodium chlorate production, electroflotation devices, battery materials and impressed current cathodic protection systems. Table 6 shows the relative attributes and costs of ceramic and metal electrodes. Some of the more important applications of Ebonex® electrodes are discussed in the remaining sections of this paper and are summarised in Table 7.

### 6.1. *Electrowinning*

Large Ebonex® electrodes are currently being developed to replace lead/silver anodes from zinc electrowinning baths. In addition to cost reduction, this will have many environmental advantages, such as re-

*Table 4. Some standard redox potentials observed on uncoated Ebonex® electrodes [11]*

| *Redox couple* | $E_e^\circ$ *vs SCE* /mV | $E_p^c$ *vs SCE* /mV | $E_p^a$ *vs SCE* /mV | $\Delta E_p$ /mV |
|---|---|---|---|---|
| [Fe(III)EHPG]$^-$/[Fe(II)EHPG]$^{2-}$ * | −580 | −900 | −380 | 520 |
| $Fe(CN)_6^{3-}/Fe(CN)_6^{4-}$ | 240 | −400 | 560 | 960 |
| Ce(IV)/Ce(III) | 1210 | −150 | – | – |

* Ligand: ethylenebis-(2-hydroxyphenylglycine), $E_e^\circ = -500$ mV *vs* SCE.

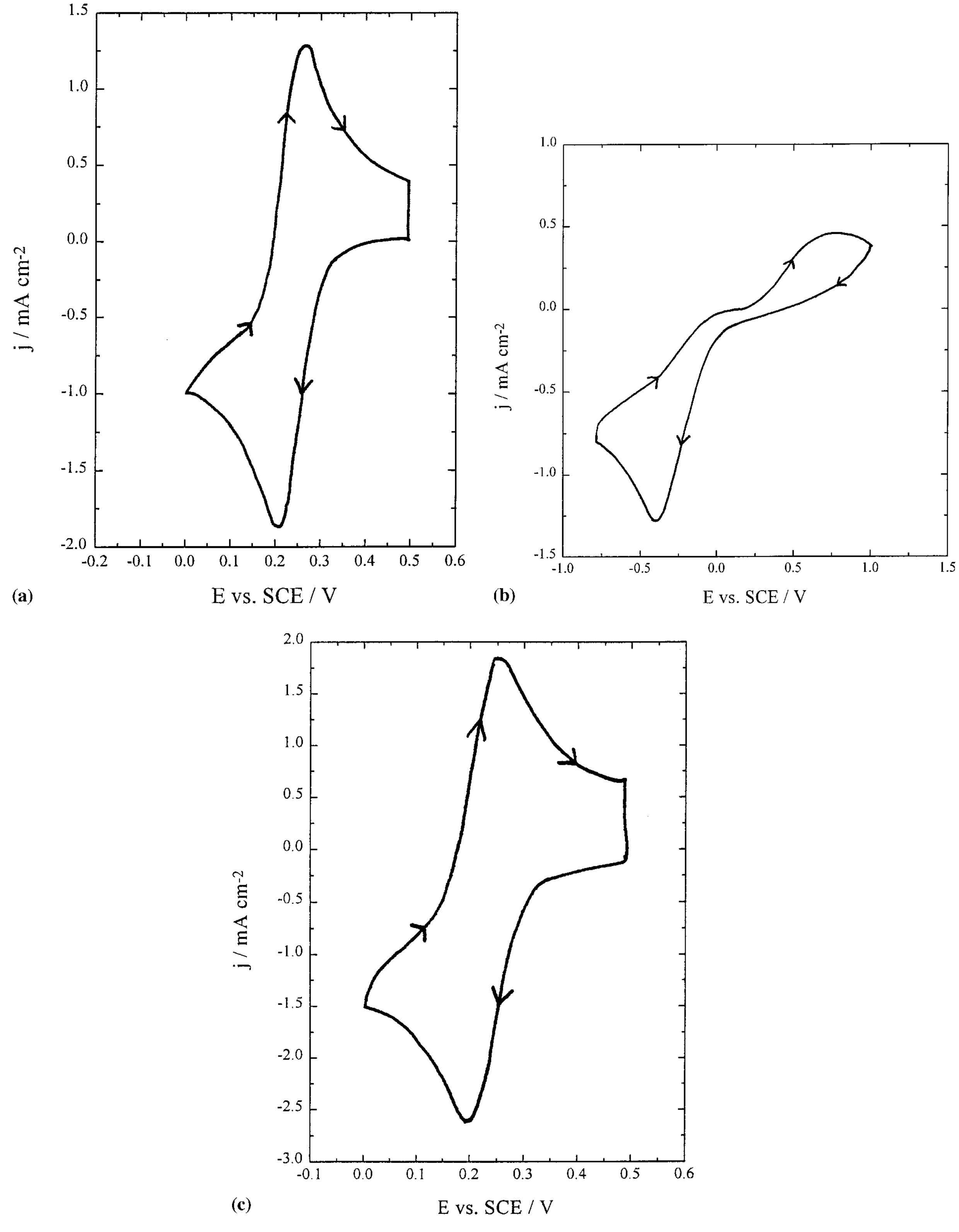

Fig. 9. Electrochemical behaviour of ferricyanide ion (10 mmol dm$^{-3}$) in potassium chloride (1 mol dm$^{-3}$) at (a) platinum, (b) Ebonex® and (c) platinum (2.4 $\mu$m) coated/Ebonex®. $\mathrm{d}E/\mathrm{d}T = 100\,\mathrm{mV\,s^{-1}}$; $T = 298\,\mathrm{K}$ [11].

moving lead from the final effluent and lead oxide dusts from around the process plant. The product, lead-free zinc, would be more desirable in car body manufacture, an important market for zinc, than that currently being produced, since lead contamination of zinc coatings can interfere with the painting processes used. Lower electrode potentials and narrower cell gaps would also reduce the electrical costs by an estimated 25%.

### 6.2. *Electroplating*

Regeneration of hard chrome plating solutions with lead dioxide coated Ebonex® electrodes prolongs

*Table 5. Typical electroplating bath conditions for the deposition of metals on Ebonex® [11]*

| *Metal* | *Plating solution* | *Plating control* | *Average coating thickness* |
|---|---|---|---|
| Cu | 75 g $dm^{-3}$ copper sulphate<br>2.2 mol $dm^{-3}$ $H_2SO_4$<br>50 mg $dm^{-3}$ $Cl^-$<br>1 g $dm^{-3}$ polyethylene glycol<br>6 mg $dm^{-3}$ DS4 | $j = 10$ mA $cm^{-2}$ | 1–100 μm |
| Au | 8.2 g $dm^{-3}$ Au as $KAu(CN)_6$<br>25 g $dm^{-3}$ citric acid, $NH_3$, pH 4 | $j = 1$ mA $cm^{-2}$ | 0.1–20 μm |
| Ni | 300 g $dm^{-3}$ $NiSO_4$<br>35 g $dm^{-3}$ $NiCl_2$<br>40 g $dm^{-3}$ boric acid, $H_2SO_4$, pH 3.5 | $j = 20$ mA $cm^{-2}$ | 100 μm |
| Pd | 10 mmol $dm^{-3}$ $PdCl_2$<br>1 mol $dm^{-3}$ KCl, HCl, pH 3 | $E = -50$ mV *vs* SCE | 1–5 μm |
| Pt | 10 mmol $dm^{-3}$ chloroplatinic acid<br>1 mol $dm^{-3}$ HCl | $E = -200$ mV *vs* SCE | 1–3 μm |

bath operation [46] and reduces the amount of chromic acid escaping into the environment. Replacement of lead anodes used in the plating process eliminates the formation of lead chromate in the bottom of plating tanks and also prolongs the use of plating solutions [26].

### 6.3. *Batteries and fuel cells*

In lead-acid batteries, Ebonex® powder and fibres have been shown to enhance formation and to improve the active mass utilization of the positive active paste [47]. Improvements in the available capacity of 15–17% have been observed for pasted flat-plate automotive-type batteries containing low levels of Ebonex® fibres. The inclusion of this ceramic is believed to enhance connectivity of the active $PbO_2$ material and act as a reinforcement to the active mass thereby aiding retention of form and porosity during cycling.

Composite cathode materials typically contain graphite and/or carbon as conductivity additives. In lithium ion batteries, use of these carbonaceous materials can lead to losses in capacity upon repetitive cycling due to intercalation with the lithium ion. Ebonex® electrodes have been shown to inhibit intercalation of the lithium ion and thereby reducing capacity losses [48]. The ability to prepare porous conductive ceramic electrodes which are highly corrosion resistant has resulted in these materials being considered in research projects for fuel cell applications.

In alkaline-manganese batteries, the active material, manganese dioxide ($MnO_2$), has a rutile structure and is therefore isomorphous and compatible with Ebonex® electrodes. Use of $TiO_2$ as an additive to the cathode has been shown to improve rechargeability [49] and to improve the capacity of primary cells by improving ionic mobility of the electrolyte species [50]. Ebonex® particulate materials offer advantages over $TiO_2$ due to their much higher conductivity, thus enabling the material to also act as a conductivity additive.

Work is also progressing in developing Ebonex particulate in plastic composite materials which show great promise as bipolar electrode substrates for batteries, especially lead–acid. Conductivities in excess of 5 S $cm^{-1}$ have been demonstrated, coupled with corrosion stability over the full range of potentials expected in such an environment.

### 6.4. *Impressed current cathodic protection anodes*

Ebonex® ceramic electrodes are being used in the protection of underground storage tanks in the USA. Steel tanks have been used to store inflammable

*Table 6. General comparison of electrode attributes and costs: ceramic vs metal [26]*

| *Attribute* | *Magnéli phase solide ceramic* | *Relative cost* | *Metal and coated metal* | *Relative cost* |
|---|---|---|---|---|
| Corrosion resistance | good | low | poor | high |
| Reversibility | yes | low | no | low |
| Base material manufacture | batch | high | – | low |
| Total production volume | low | high | high | low |
| Production capital investment | high | high | high | low |
| Energy needs | high | high | high | low |
| Ease of fabrication | low | high | high | low |
| Ease of connection | low | high | high | low |
| Large sizes | yes | high | yes | low |
| Current feed | poor | high | good | low |
| Robustness | low | high | high | low |

*Table 7. Some industrial applications for porous uncoated and coated Ebonex® electrodes* [*26*]

| *Coating type* | *Application* | *Electrolyte, aggressive component* | *Maximum recorded current density* /A $m^{-2}$ |
|---|---|---|---|
| Uncoated | Water sterilization | Water | 1 |
| | Electrochlorination | Chloride ion | 1 |
| | Cathodic protection | Acid/oxygen/fluoride ion | 1 |
| | Electrophoresis | Oxygen evolution | 1 |
| | Dewatering | Reversible | 1 |
| | Batteries | Oxygen/acid/alkali | 5–20 |
| | Electrosynthesis | Application dependant | 1–20 |
| Iridium oxide | Etchant recycling | Mineral acids + 1% fluoride | 20 |
| | Metal recovery | Various acids | 20 |
| | Electrowinning | Fluoride | 20 |
| | Electroplating | Fluoroborate etc EDTA | 20 |
| | Electrochlorination | Swimming pools | 5 |
| | (reversible) | Seawater | 20 |
| Platinum, thermal or plated | Electrosynthesis | Possible inactivation of platinum by organic compounds | 20 |
| | Metal finishing | Chromic acid | 20 |
| | | Cyanide | 20 |
| Platinum/Iridium | Electrochlorination | – | 20 |
| | Chlor-alkali bipoles | | 40 |
| Ruthenium dioxide/ | Cathodic protection | Acid/oxygen | 20 |
| titanium dioxide | Chlor-alkali bipoles | Chlorine gas attrition/hydride formation resistance | 40 |
| $RuO_2/IrO_2TiO_2$ | Chlor-alkali bipoles | Chlorine gas attrition/hydride formation resistance | 20–40 |
| | Electrochlorination | Reversible operation | |
| Lead dioxide | Hexavalent chromium regeneration | Hard chrome plating solutions, fluoride | 20 |
| | Anodising solutions | Fluoride | 20 |
| | Organic waste destruction | Chloride, nitrate | 10 |
| | Ozone generation | Water, phosphate or fluoroborate | 10 |
| | Redox regeneration | Fluoride, nitrate, chloride | 20–30 |
| | HCl electrolysis | Bipolar operation | 20 |
| Tin dioxide | Anodic oxidations | | 10 |
| | Organic waste destruction | | 10 |

materials, mainly petroleum products since the late 1800s. Many are leaking through corrosion and contaminating aquifers. Of the leaking tanks inspected, 70% are suffering from external corrosion which could have been prevented by cathodic protection. One million of an estimated 3–5 million tanks in use in the USA have been reported to be leaking one hundred million gallons of product every year, presenting a significant environmental problem.

Ebonex® rod electrodes, about 90 cm long and 5 mm diameter, have been used as cathodic protection anodes for this process. The following factors were taken into consideration for the design of these electrodes: (a) anodes in soil develop an acidic environment, often hydrochloric acid, sulphuric acid and nitric acid and combinations, since diffusion of anions from the electrode is inhibited; Magnéli phase ceramics are tolerant to these conditions; (b) narrow section electrodes are easy and inexpensive to install; (c) iridium oxide coated Ebonex® electrodes have a long life at the low current densities required for these operations. Hundreds of rod electrodes in various types of soil and location are currently in use and show no signs of failure since their installation in 1990. New systems using Ebonex® materials are being developed in the UK and Australia for cathodic protection of metals in concrete and for marine applications [26].

### 6.5. *Electrochemical soil remediation*

Ebonex® electrodes are being developed for use as stable noncontaminating collector electrodes for detoxification of land by electrokinetic movement of ions and water. It has been reported that over 50 000 industrial sites in the UK are contaminated by industrial processing [51]. Much of this contamination is due to heavy metals such as lead, cadmium, arsenic (from wood preservatives in timber yards), chromium (in the form of chromic acid from metal finishers and tanneries), zinc (from steel galvanizing) and many others. In the Netherlands, a comparatively small country, a land clean-up bill of $25 billion over the next 25 years has been estimated [52]. The EEC commission estimates the clean-up bill for its member states to be $64 billion [53]. One of the most useful and economical ways to remediate land is to collect the metals and acid anions electrochemically, using buried anodes and cathodes strategically placed about 1.5 m apart, to depths of 3 m or more [54]. Soil, as with wet concrete, behaves as an aqueous electrolyte and ions and water are free to migrate towards electrodes. Soil that contains as little as 10% moisture can provide a continuous path for ions. Cations, such as metal ions and the ammonium ion, and soluble organic materials that are positive charged move towards the cathode under the influence of a d.c. current. Anions such as chloride, fluoride, nitrate, arsenate and negatively charged organic materials move towards the anode. By arranging the electrodes in collector vessels it is possible to collect these ions and process the water for return to the soil. The process is operated until the concentration of toxic ions is reduced to an acceptable level, usually taking between 60–120 days. Average ion velocity is about 0.08–0.16 m day$^{-1}$ at a typical current density of 2–8 A m$^{-2}$. The process cannot be rushed since increasing the flux tends to dry out the soil due to the joule heating effect. A further problem is caused by the distortion of the pH around the anodes and cathodes which cannot be relieved by mixing of the electrolyte. Soil/water management is an essential part of the process. In many instances this *in situ* soil remediation process is competitive with all other types of remediation processes other than denial and/or dumping in landfill, currently the preferred options. Assuming that electrodes are recoverable, which is very likely with Ebonex® materials, the electricity cost is in the region of 100–800 kW h m$^{-3}$ (£7–£56 per m$^3$ with electricity costs of £0.07 per kW h).

Ebonex® electrodes may also find application as inert electrodes in bioremediation and *in situ* digestion processes for the removal of toxic organics from waste solutions and sewage streams.

### 6.6. *Oxidation of organic wastes including sewage*

Direct electrochemical oxidation of drinking water with Ebonex® electrodes has recently been studied [11, 34, 55]. Destruction of organic waste streams has been demonstrated using Ebonex® particulate packed beds coating with lead dioxide or tin oxide [56]. This technology is part of an effort to deal with faecal matter and urine in space stations and other remote locations. Studies have been carried out to determine the effect of anodic particle size, flow rate of faeces/urine mixture, packed bed height, current density and cathode to anode spacing arrangement, on the rate of human waste oxidation. It has been shown that Ebonex® particulate (0.5–1.0 mm diameter) coated with $SnO_2/Sb_2O_3$, a solution flow rate of 0.9–1.4 cm s$^{-1}$ through a packed bed based on the cross-sectional area of the reactor, a bed height of 5.8 cm and a current density based on the geometric area of the particle of 5 mA cm$^{-1}$ comprise an optimum set of parameters for the scale-up of a packed-bed electrochemical reactor system [57]. Electrochemical incineration is attractive as the products are water, carbon dioxide and hydrogen which are useful. The technology is attractive for marine, aviation, railways and polar regions where bacterial digestion in conventional sewage plants is too slow to be useful.

### 6.7. *Flexible conductors*

Traditionally, carbon blacks have been used as fillers in energy cables to provide low levels of conductivity. This is necessary to attenuate local magnetic spikes in the insulating sheath which reduce the service life of energy cables. Conductive plastics incorporating Ebonex® type powders as fillers offer advantages over carbon black materials, including rigidity and resistance to oxidation [58, 59]. One surprising feature of the plastic composites is the compatibility between the Magnéli phase powders and the organic phase. It is possible, for example, to weld polyethylene filled Ebonex® materials to themselves and also to unfilled polyethylene. These composite materials can be extruded to form wires and cables for electromagnetic shielding applications.

### 6.8. *Electrophoresis*

Ebonex® ceramic electrodes are of interest in electrophoretic applications due to the unique combination of conductivity and corrosion resistance, coupled with their ability to withstand polarity reversal [26]. The electrodes are noncontaminating owing to their inertness in a wide-range of electrolytes; graphite, for example, oxidises as an anode and will cause contamination or ‘sloughing’ of the electrolyte and precious metals are susceptible to attack in certain organic electrolytes. Ceramic electrodes permit a wide flexibility in the choice of gel type and format due to their chemical inertness, especially to organic electrolytes. They provide consistent, high speed, high resolution separations due to the generation of a strong, uniform electric field. The material provides excellent voltage and current distribution owing to its high surface area and offers excellent performance in reverse fields or pulsed electrophoresis because of their unparalleled polarity reversal stability. In rod form, the electrodes have the requisite properties for electrophoretic separation; the material is durable, easily cleaned and maintained. High voltage electrophoretic applications will often exceed the breakdown potential of currently available electrode materials, such as titanium, causing dissolution into the electrolyte. The use of this material eliminates this problem since it can be operated at significantly higher voltages than other electrodes without degradation.

Other potential biotechnology uses include DNA sequencing, electroelution, gene splitting, biosensors, biomedical equipment, pacemakers, implants, electrochemical bone growth stimulation and drug delivery systems.

## 7. Summary

Magnéli phase titanium oxide ceramic electrodes, commercially known as Ebonex® materials, are beginning to challenge precious metal coated and carbon electrodes in many industrial applications. They are particularly stable to aggressive environments where conventional electrode materials are more readily attacked. The electrochemical properties of Ebonex® materials can be further improved by coating with a suitable metal or metal oxide. The challenge ahead will be to produce the materials in rugged forms for large scale industrial applications to provide new materials for batteries, fuel cells, electrosynthesis cells, electrochemical devices and soil remediation. The ability to produce flexible electrodes by compounding Ebonex® powders in a polymer matrix to filling efficiencies in excess of 85% by weight will allow problems associated with the processibility of these advanced electrode materials to be overcome in the near future.

## Acknowledgements

The authors are grateful to K. Ellis and A. Hill at Atraverda Ltd (Sheffield, UK) and D. Brackenbury at Electrochemical Design Associates (Gainsborough, UK) for supplying Ebonex® materials. Assistance with early literature searching was provided by I. George.

## References

[1] S. Andersson, *Acta Chem Scand.* **11** (1957) 1641.
[2] R. L. Clarke and S. K. Harnsburger, *Am. Lab.* **20** (1988) 6.
[3] J. F. Houlihan and L. N. Mulay, *Phys. Stat. Sol. B* **61** (1974) 647.
[4] R. F. Bartholomew and D. R. Frankl, *Phys. Rev.* **187** (3) (1960) 828.
[5] J. F. Houlihan and L. N. Mulay, *Mater. Res. Bull.* **6** (1971) 737.
[6] J. B. Goodenough, *ibid.* **2** (2) (1967) 165.
[7] L. K. Keys and L. N. Mulay, *J. Appl. Phys.* **38** (1967) 1466.
[8] D. Goldschmidt and M. Watanabe, *Mater. Res. Bull.* **20** (1985) 65.
[9] R. J. Pollock, J. F. Houlihan, A. N. Bain and B. S. Coryea, *ibid.* **19** (1984) 17.
[10] R. R. Miller-Folk and R. E. Noftle, *J. Electroanal. Chem.* **274** (1989) 257.
[11] J. E. Graves, D. Pletcher, R. L. Clarke and F. C. Walsh, *J. Appl. Electrochem.* **21** (1991) 848.
[12] J. K. Burdett and J. F. Mitchell, *Chem. Mater.* **5** (1993) 1465.
[13] M. Amjad and D. Pletcher, *J. Electroanal. Chem.* **59** (1975) 61.
[14] D. P. Sepa, A. Damjanovic and J. O'M. Bockris, *Electrochim. Acta* **12** (1967) 746.
[15] S. Andersson, A. Sundholm and A. Magnéli, *Acta Chem. Scand.* **13** (1959) 989.
[16] G. V. White *et al.*, Ceramics, Adding the Value, Proceedings of the International Ceramic Conference, Austceram '92, Vol. 1, (1992), p. 365.
[17] H. Anderson and P. Hyde, *J. Phys. Chem. Solids* **28** (1967) 1392.
[18] Atraverda Ltd., Darenth House, Rotterham Road, Eckington, Sheffield, S31 9FH, UK, company literature (1995).
[19] M. Marezio, D. McWhan, P. Derniero and J. Remeica, *J. Solid State Chem.* **6** (1973) 213.
[20] K. Nagarawa, Y. Kato and Y. Bando, *J. Phys. Soc. Jpn.* **29** (1970) 241.
[21] L. K. Keys and L. N. Mulay, *Phys. Rev.* **154** (1967) 453.
[22] L. N. Mulay and W. J. Danley, *J. Apply. Phys.* **41** (1970) 877.
[23] W. J. Danley and L. N. Mulay, *Mater. Res. Bull.* **7** (1972) 739.
[24] C. Schlenker, R. Buder, M. Schlenker, J. F. Houlihan and L. N. Mulay, *Phys. Stat. Sol. B.* **54** (1972) 247.
[25] J. B. Goodenough, 'Progress in Solid Chemistry' Vol. 5 (edited by H. Reiss), Pergamon Press, New York (1971).
[26] R. L. Clarke, 2nd European Conference on Electrochemical Processing. Innovation and Progress, Moat House International, Glasgow, 21–23 Apr. (1993).
[27] K. Kohlbrecka and J. Przyluski, *Electrochim. Acta* **39** (11/12) (1994) 1591.
[28] R. L. Clarke and R. Pardoe, 'Application of Ebonex® Conductive Ceramic Electrodes in Effluent Treatment in Electrochemistry for a Cleaner Environment' (edited by J. D. Genders and N. L. Weinberg), The Electrosynthesis Company, New York (1992).
[29] A. M. Couper, D. Pletcher and F. C. Walsh, *Chem. Rev.* **90** (1990) 837.
[30] P. C. S. Hayfield, *US Patent 4 422 917* (1983).
[31] S. M. Jasem and A. C. C. Tseung, *J. Electrochem. Soc.* **126** (8) (1979) 1353.
[32] J. D. C. Haenen, W. Vischer and E. Barendrecht, *J. Appl. Electrochem.* **15** (1985) 29.
[33] B. E. Conway and T. C. Liu, *Phys. Chem.* **91** (1987) 4610.
[34] J. E. Graves, D. Pletcher, R. L. Clarke and F. C. Walsh, *J. Appl. Electrochem.* **22** (3) (1992) 200.
[35] Atraverda Ltd., Sheffield (see [18]), company literature (1996).
[36] C. J. Brown, D. Pletcher, F. C. Walsh, J. K. Hammond and D. Robinson, *J. Appl. Electrochem.* **24** (1994) 95.
[37] P. Trinidad and F. C. Walsh, *Electrochim. Acta* **41** (4) (1996) 493.
[38] F. C. Walsh, unpublished work.
[39] J. R. Smith, A. H. Nahlé and F. C. Walsh, *J. Appl. Electrochem.* **27** (7) (1997) 815.
[40] BS. EN. 623-2, 'Advanced Technical Ceramics – Monolithic Ceramics – General and Textural Properties. Part 2: Determination of density and porosity,' CEN European Committee for Standardization, Brussels, Sept. (1993).
[41] K. Ellis, Atraverda Ltd., personal communication.
[42] Electrochemical Design Associates (EDA), 'Recent Developments in Ebonex® Electrodes: Cable Electrodes', company literature, EDA Technology, 829 Heinz street, Berkeley, CA 94710, USA (1996).
[43] P. C. S. Hayfield and R. L. Clarke, *in* Proceedings of the Electrochemical Society Meeting, Los Angels, 7–12 May (1989).
[44] L. He, H. F. Franzen, J. E. Vitt and D. C. Johnson, *Electrochem. Soc.* **141** (4) (1994) 1014.
[45] S.-Y. Park, S.-I. Mho, E. O. Chi, Y. U. Kwon and H. L. Park, *Thin Solid Films* **258** (1995) 5.
[46] M. Mayr, W. Blatt, B. Busse and H. Heinke, 4th International Forum on Electrolysis in the Chemical Industry, Fort Lauderdale, FA, Nov. (1990).
[47] CSIRO Report DMR-098, 'Evaluation of the Effect of Ebonex® Additive on Lead–acid Battery Capacity at Different Discharge Rates', Aug. (1995).
[48] W. J. Macklin and R. J. Neat, *Solid State Ionics* **53–56** (1992) 694.
[49] K. Kordesch, J. Gsellmann and T. Klaus, *World Patent PCT Int. Appl. WO 90 02 423* (1990).
[50] J. E. Mieczkowska and S. P. Markfort, *US Patent 5 342 712* (1994).
[51] S. Timothy, 'Contaminated Land: Markets and Technology Issues', Centre for Exploitation of Science and Technology, 5 Bemers Road, Islington, London (1992).
[52] Department of Trade and Industry, Overseas Trade Services, 'Soil Contamination Cleaning up in the Netherlands', Earls Court, London, 15 Oct. (1992).
[53] M. R. G. Taylor and R. A. N. McLean, 'Overview of Cleaning-up Methods for Contaminated Sites', London Waste Authority (1992).
[54] R. Lageman, 'Electro-reclamation', *Chem. Ind.*, 18 Sept. (1989) 585.

[55] Department of the Environment, Contract PEPCD 7/7/138, Jan. (1991).

[56] J. O'M. Bockris, 'Environmental Applications of Electrochemical Technology', 6th International Forum on Electrolysis in the Chemical Process Industries, Nov. (1993).

[57] C. L. K. Tennakoon, R. C. Bhardwaj and J. O'M. Bockris, *J. Appl. Electrochem.* **26** (1996) 18.

[58] R. L. Clarke and R. Pardoe, 4th International Forum on Electrolysis in the Chemical Industry, Fort Lauderdale, FA, Nov. (1990).

[59] D. Brackenbury, R. L. Clarke, J. Vinson and F. C. Walsh, '*Recent Developments in Ebonex® Electrodes*', 5th International Forum on Electrolysis in the Chemical Industry, FA, Nov. (1996).